Materials Science and Engineering A 442 (2006) 336-341.

Elasticity study of very thin Cu films

K. Fujiwara, H. Tanimoto and H. Mizubayashi*
Institute of Materials Science, University of Tsukuba, Tsukuba, Ibaraki 305-8573, Japan

Abstract

The elastic property and the surface morphology of Cu/Ta films and Ta/Cu/Ta films sputter-deposited on Si reed substrates were studied for the Cu film thickness, t_{Cu}, between 7 and 1000 nm. A monotonic increase in the internal friction, $Q^{-1}{}_f$, in the constituent Cu film above 200 K was commonly observed. For Cu/Ta films, Young's modulus of a Cu film, E_f, showed good agreement with the theoretical value for t_{Cu} > ~80 nm and a decrease with decreasing t_{Cu} below ~80 nm. A decrease in $Q^{-1}{}_f$ after 400 K annealing, $\Delta Q^{-1}{}_{f,400K}$, and the surface roughness showed the local minimum and the local maximum near 80 nm, respectively, indicating that the properties of the Cu film were modified by subsequent deposition of a Cu layer (the self capping effect). For Ta/Cu/Ta films, Ta capping brought about an increase in the grain size parallel to the film surface, a decrease in the internal stress and a decrease in E_f but no changes in the grain size normal to the film surface, $Q^{-1}{}_f$, $\Delta Q^{-1}{}_{f,400K}$ and the outline of the surface roughness. These results are discussed in the light of the anelastic responses of grain boundaries and interface in nano-scale Cu films which may be important for down sizing of electric devices.

Keywords: Cu thin film, Young's modulus, Internal friction, Internal stress, Surface morphology, Capping effect
*Corresponding author. E-mail: mizubayashi@ims.tsukuba.ac.jp

1. Introduction

Understanding of the elastic property of nm-scale Cu interconnects is important for the semiconductor devices because the internal stress induced in Cu/low-dielectric-constant-material interconnects will be a serious issue because the low-dielectric-constant materials tend to be mechanically weak [1,2]. Further, electromigration and stress-induced migration (stressmigration) failures are of the most important issue in metallization, where the film thickness dependence of Young's modulus, the internal stress, the crystallographic texture, the grain size and the property of the grain boundaries should be understood [2-4], because the electromigration and stressmigration failures at the device operating temperature of 100 ºC in real devices are induced by surface and/or interface diffusions [1]. In nanostructured metals, the fractional volume of the grain boundary regions and the surface and/or interface regions increase with decreasing grain size, film thickness and/or interconnect size. For nanostructured thin films and/or specimens of Al [5-7], Cu [8,9] Au [10,11], the grain boundary anelastic process (GBAP) is thermally activated above 200 K and causes an increase in the internal friction and a considerable

decrease in Young's modulus. On the other hand, the internal friction peak due to the GBAP in bulk Cu is observed near 500 K [12], indicating that the atomic process in nanostructured Cu may be not in the extension from that in bulk Cu. For the atomic transports in the surface and/or interface regions in nm-scale Cu films, it has been reported that capping of Cu films brings about the elongation of the lifetime of electromigration failure [13] and the suppression of the diffusional creep [14] and the internal stress relaxation [15]. The underlying mechanisms for these characteristic phenomena are, however, not clear yet because of a lack of the experimental knowledge concerned.

Recently it was reported that for a Cu film on a Ta buffer layer deposited by sputtering, Young's modulus of the Cu film showed a decrease with decreasing Cu film thickness below about 100 nm [8]. It was further reported for the Cu film on a Ta buffer layer that the surface roughness showed the maximum at around $t_{Cu} \approx 80$ nm and the decrease of the internal friction caused by 400 K annealing showed the minimum at around $t_{Cu} \approx 80$ nm, where t_{Cu} is the Cu film thickness [16]. In the present study, we investigated an effect of Ta capping on the characteristic elastic property and surface morphology found for a Cu film on a Ta buffer layer because Cu films and interconnects in real devices are always capped by a buffer layer.

2. Experiment

For the composite reed of a thin film on a reed-substrate, Young's modulus, E_f, and the internal friction, $Q^{-1}{}_f$, of the film may be given by the following equations [5,6],

$$E_f = (E_s/3)[2(\Delta f_f/f_s)/(t_f/t_s)+(\rho_f/\rho_s)][(1-\nu_f^2)/(1-\nu_f\nu_s)] \quad (1)$$

$$Q^{-1}{}_f = \Delta Q^{-1}{}_f (t_s/3t_f)(E_s/E_f) \quad (2),$$

where the subscripts of "f " and "s" denote the quantities for the film and the reed substrate, respectively. E, t, ρ and ν denote Young's modulus, the film thickness, the density and Poisson ratio, respectively. In the present setup, the reed-substrate was a Si reed-substrate with a Ta buffer layer. $\Delta f_f/f_s$ and $\Delta Q^{-1}{}_f$ were defined as $(f_{s+f} - f_s)/f_s$ and $(Q^{-1}{}_{s+f} - Q^{-1}{}_s)$, where f_s and $Q^{-1}{}_s$ were the resonant frequency and the internal friction of the reed-substrate with a Ta buffer layer, and f_{s+f} and $Q^{-1}{}_{s+f}$ were the resonant frequency and internal friction of the composite reed of a Cu thin film on the reed substrate, respectively.

Figure 1(a) is a schematic drawing of a silicon reed-substrate with a thick end for clamping. A silicon reed-substrate was chemically etched and terminated by hydrogen prior to the metallization. Figure 1(b) is a schematic drawing of a measurement setup. The metallization was conducted by dc-sputtering at room temperature in Ar (6 N purity) at $1.3\text{x}10^{-1}$ Pa, where the deposition rate of Cu and Ta was 5 and 2 nm/min, respectively. Figure 1(c) shows schematic cross sectional views of a Cu/Ta film and a Ta/Cu/Ta film. Firstly a 30 nm Ta buffer layer (Ta-1 in Fig. 1(c)) was deposited on a Si reed substrate and the resonant frequency, f_0, of the Si reed substrate with the Ta-1 layer was measured as shown in Figure 2(a). Then an additional Ta buffer layer (Ta-2 in Fig. 1(c)) and a Cu specimen film were deposited for a Cu/Ta film. For a Ta/Cu/Ta film, the Ta-2 layer, a Cu specimen film and a Ta cap layer (Ta-3 in Fig.(c)) were sequentially deposited. The thickness of the Ta-2 buffer layer was 30 nm for the Cu/Ta films with the Cu film thickness, t_{Cu}, more than 30 nm and was 5 nm for the thinner Cu/Ta films and all the Ta/Cu/Ta films, respectively. The thickness of the Ta-3 cap layer was 5 nm. A change in the resonant frequency, Δf_{Ta}, of a Si reed substrate due to deposition of the Ta-2 and the Ta-3 layers was separately calibrated. Figure 2(b) shows examples of Δf_{30nmTa} observed for deposition of the 30 nm Ta-2 layer, where data $\Delta f_{30nmTa} = 0.3215 \pm 0.0173$ Hz was found. In Fig. 2(a), the resonant frequency, f_1, of the Si reed substrate

after deposition of the 30 nm Ta-2 buffer layer and the 40 nm Cu film is shown. It is noted that f_{s+f} and f_s in Eq. (1) are determined as f_1 and (f_0 + Δf_{30nmTa}) in Fig. 2(a), respectively or Δf_f = $\Delta f_{1\text{-}0}$ - Δf_{30nmTa} for a Cu/Ta film. It is not shown here but the calibrations for Δf_{5nmTa} and $\Delta Q^{-1}{}_{Ta}$ were also made separately.

The X-ray diffraction (XRD) measurement was performed with the Cu-Kα radiation. The scattering vector was normal to the surface of a Cu film and the reflections from Si powders put on the film surface were used as reference. The surface morphology of Cu/Ta and Ta/Cu/Ta films was observed by using the STM operating in the constant current mode at the atmosphere.

3. Results

In Figures 3(a) to 3(c), the fractional intensity of the XRD Cu200 reflection, $I_{200}/(I_{111}+I_{200})$, the mean grain size, $D_{\perp(111)}$, in a Cu film and the (111) plane spacing normal to the surface of a Cu film, $d_{\perp(111)}$, are plotted as a function of the Cu film thickness, t_{Cu}, respectively. For the Cu/Ta films [16], the strong <111> texture was observed for t_{Cu} thinner than about 100 nm and then I_{200} started to increase with increasing t_{Cu} above about 100 nm. It is noted that the strong <111> texture was reported commonly for sputter deposited Cu/Ta films [4,17,18]. For the Ta/Cu/Ta films, the values of $I_{200}/(I_{111}+I_{200})$ appeared to be constant about 0.2 in the present t_{Cu} range from 20 to 300 nm. It is noted that such change in $I_{200}/(I_{111}+I_{200})$ was induced by Ta capping. For both the Cu/Ta and Ta/Cu/Ta films, $I_{200}/(I_{111}+I_{200})$ remained unchanged after annealing at 400 K.

In Fig. 3(b), $D_{\perp(111)}$ was estimated from the peak width of the (111) reflection and the Scherrer's equation, where the experimental resolution for the upper bound of $D_{\perp(111)}$ was about 100 nm. For both the Cu/Ta films and the Ta/Cu/Ta films in the as deposited state, $D_{\perp(111)}$ increased gradually to about 100 nm with increasing t_{Cu} to 1000 nm. For the Cu/Ta films, 400 K annealing hardly changed $D_{\perp(111)}$ for t_{Cu} thinner than 100 nm and appeared to cause a slight increase in $D_{\perp(111)}$ for t_{Cu} thicker than 100 nm. For the Ta/Cu/Ta films, $D_{\perp(111)}$ showed almost no change after annealing at 400 K.

As seen in Fig. 3(c), with decreasing t_{Cu}, $d_{\perp(111)}$ showed a gradual decrease for the Cu/Ta films and remained almost unchanged for the Ta/Cu/Ta films, respectively. The internal tensile stress along the Cu film surface, $\sigma_{i//}$, determined from the $d_{\perp(111)}$ data are shown together, where a change in $d_{\perp(111)}$ from its reference value was assumed to be the Poisson contraction or expansion. As already mentioned for $I_{200}/(I_{111}+I_{200})$, Ta capping caused a decrease in $\sigma_{i//}$ too.

Figure 4 shows the E_f *vs*. t_{Cu} data observed for the Cu/Ta and Ta/Cu/Ta films, where the experimental errors were mainly associated with those in the calibrations for Δf_{Ta}. For the Cu/Ta films [16], E_f was almost the same to $E_{<110>}$ for t_{Cu} > ~80 nm and gradually decreased with decreasing t_{Cu} below ~ 80 nm, where the E_f *vs*. t_{Cu} data for t_{Cu} > ~80 nm were well explained by the theoretical values of E_f estimated by taking into account the crystallographic texture (Fig. 3(a)) [7] and the internal stress (Fig. 3(c)) [19].

The values of E_f observed for t_{Cu} < ~ 80 nm was lower by ~2×10^{10} Pa than the theoretical values of E_f. Such decrease in E_f may be attributed to GBAP [7-11]. On the other hand, as seen for the Ta/Cu/Ta films, Ta capping caused a decrease in E_f which was stronger with decreasing t_{Cu}. In other words, after Ta capping, the observed values of E_f were considerably lower than the theoretical values of E_f, especially for t_{Cu} < ~ 80 nm.

Figure 5 shows examples of the Q^{-1} spectra observed for a Si reed substrate with a 30 nm Ta buffer layer alone and for a Si reed-substrate with a 300 nm Cu specimen film on a 30 nm Ta buffer layer (Cu/Ta). For the Si reed substrate with a Ta buffer layer alone, the Ta buffer layer was responsible for a small Q^{-1} peak at ~200 K and the gradual increase in Q^{-1}

above ~250 K was due to the thermoelastic relaxation of the Si reed substrate [6]. After the deposition of the Cu specimen film, Q^{-1} showed a strong and monotonic increase above ~200 K due to GBAP as already mentioned. $Q^{-1}{}_{f}$ of the Cu film was determined from $\Delta Q^{-1}{}_{Cu}$ shown in Fig. 5 and Eq. (2). For the as deposited Cu/Ta film, $Q^{-1}{}_{f}$ showed a considerable decrease between 350 K and 400 K which was monitored as a decrease in Q^{-1} at 300 K after annealing at 400 K, $\Delta Q^{-1}{}_{Cu,400K}$, as shown in Fig. 5.

Figure 6(a) shows the $Q^{-1}{}_{f}$ *vs.* t_{Cu} data observed for the Cu/Ta and Ta/Cu/Ta films, where the experimental errors in the $Q^{-1}{}_{f}$ data were mainly associated with those in the calibrations for $\Delta Q^{-1}{}_{Ta}$. $Q^{-1}{}_{f}$ at 300 K was about 6×10^{-3} in the Cu/Ta films and was hardly modified by Ta capping. Figure 6(b) shows the $\Delta Q^{-1}{}_{f,400K}$ *vs.* t_{Cu} data observed for the Cu/Ta and Ta/Cu/Ta films. For the Cu/Ta films, $\Delta Q^{-1}{}_{f,400K}$ showed a gradual increase when t_{Cu} leaved from ~80 nm, i.e. a local minimum near 80 nm. As seen for the Ta/Cu/Ta films, the $\Delta Q^{-1}{}_{f,400K}$ *vs.* t_{Cu} data were hardly modified by Ta capping too.

Figures 7 (a) and 7(b) show the STM surface images observed for the Cu/Ta (t_{Cu} = 10 nm) and Ta/Cu/Ta films (t_{Cu} = 30 nm), respectively. It is noted that the relieves of pyramidal dips on the Si reed substrate due to the chemical etching were also observed, e.g., those with ~100 nm square and ~40 nm deep in Fig. 7(a) and more shallow in Fig. 7(b) due to the mild chemical etching. From the surface morphology of the Cu/Ta and Ta/Cu/Ta films, the mean crystallite size along the surface, $D_{//}$, was estimated to be ~10 nm for the Cu/Ta film and ~50 nm for the Ta/Cu/Ta film, respectively. As already mentioned, $D_{\perp(111)}$ for the Cu/Ta films was similar to $D_{//}$, and $D_{\perp(111)}$ was hardly modified by Ta capping. In other words, Ta capping modified $D_{//}$ but not $D_{\perp(111)}$. Fig. 8 shows the t_{Cu} dependence of the root mean squire (RMS) roughness observed for the Cu/Ta and Ta/Cu/Ta films, where the RMS roughness data for the bare Si reed substrate and the Si reed substrate with 30 nm thick Ta buffer layer are also indicated as a reference. The amplitude of the RMS roughness measured from that of the reference was larger for the Ta/Cu/Ta films than for the Cu/Ta films and the local maximum was commonly observed at around t_{Cu} of 80 nm.

4. Discussion

The characteristic property found for the nanostructured Cu/Ta films are the decrease in E_f for t_{Cu} < ~80 nm (Fig. 4), the local minimum of $\Delta Q^{-1}{}_{f,400K}$ at t_{Cu} of ~80 nm (Fig. 6(b)) and the local maximum of the RMS roughness at t_{Cu} of ~80 nm (Fig. 8) [16]. Both the decrease in E_f for t_{Cu} < ~80 nm and the local minimum of $\Delta Q^{-1}{}_{f,400K}$ at t_{Cu} of ~80 nm are associated with GBAP in nanostructured Cu and they are indicative of the magnitude of GBAP and the thermal stability of GBAP, respectively. The local maximum of the RMS roughness at t_{Cu} of ~80 nm indicates that the growth mechanism of a Cu film was modified by additional deposition of Cu (the self capping effect) and a change in the self capping effects took place at t_{Cu} of ~80 nm. That is, the property of the grain boundary regions in nanostructured Cu is not on the extension from that in bulk Cu and not of a monotonic function of t_{Cu}. For the Cu/Ta films, E_f showed a considerable decrease with decreasing t_{Cu} below ~80 nm although $Q^{-1}{}_{f}$ remained almost constant (Figs. 4 and 6(a)), indicating that the constituent relaxed anelastic strain was mainly responsible for the decrease in E_f. Such strong decrease in E_f due to the constituent relaxed anelastic strain has been found in nanocrystalline Au too [11].

Ta capping caused the randomize of the crystallographic texture (Fig. 3(a)), an increase in $D_{//}$ (Fig. 7(a)), a decrease in $\sigma_{i//}$ (Fig. 3(c)) and a decrease in E_f (Fig. 4). On the other hand, no changes in $D_{\perp(111)}$ (Fig. 3(b)), $Q^{-1}{}_{f}$ (Fig. 6(a)), $\Delta Q^{-1}{}_{f,400K}$ (Fig. 6(b)) and the outline of the RMS roughness (Fig. 8) are observed after Ta capping. The randomize of the crystallographic

texture (Fig. 3(a)), an increase in $D_{//}$ (Fig. 7(a)), a decrease in $\sigma_{i//}$ and no changes in $D_{\perp(111)}$ indicate that Ta capping caused the grain growth along the film surface but not along the film thickness. Then, almost no changes in $Q^{-1}{}_f$ (Fig. 6(a)) and $\Delta Q^{-1}{}_{f,400K}$ due to Ta capping indicate that GBAP under the stress parallel to the film surface were mainly associated with the grain boundaries parallel to the film surface. On the other hand, the combination of the enhancement of the decrease in E_f, the increase in $D_{//}$ and the decrease in $\sigma_{i//}$ found after Ta capping indicates that the grain boundaries and the interfaces of the lamellar like films give rise the strong relaxed-anelastic-strain. In other words, since the grain boundaries and the interfaces in the nano-scale lamellar like films and interconnects can serve as a mechanical buffer layer for the low-dielectric-constant materials [1,2]. On the other hand, however, such grain boundaries and interface may also serve as a channel for mass transport for the electromigration and stressmigration. It is reported that the electromigration failure at the device operating temperature of 100 ºC in real devices is induced by interface and surface diffusions [1]. The present work demonstrates that understanding of the anelastic responses of grain boundaries and interface in nano-scale Cu films is important for down sizing of devices.

5. Conclusion

The monotonic increase in $Q^{-1}{}_f$ above 200 K associated with GBAP was commonly observed for Cu/Ta and Ta/Cu/Ta films. For Cu/Ta films, E_f found for $t_{Cu} > \sim 80$ nm showed good agreement with the theoretical value. E_f observed for $t_{Cu} < \sim 80$ nm showed a decrease from the theoretical value and attributed to the relaxed anelastic strain associated with GBAP. A decrease in GBAP-$Q^{-1}{}_f$ after annealing at 400 K, $\Delta Q^{-1}{}_{f,400K}$, and the root mean square (RMS) surface roughness showed the local minimum and the local maximum near 80 nm, respectively, indicating that the properties of a Cu film were modified by subsequent deposition of a Cu layer (the self capping effect). For Ta/Cu/Ta films, Ta capping brought about the randomize of the crystallographic texture, an increase in the grain size parallel to the film surface, a decrease in the internal stress and a decrease in E_f but no changes in the grain size normal to the film surface, $Q^{-1}{}_f$, $\Delta Q^{-1}{}_{f,400K}$ and the outline of the RMS roughness. These results indicate that the grain boundaries and the interfaces of the lamellar like films attained after Ta capping gave rise the strong relaxed-anelastic-strain.

Acknowledgement

This work is partly supported by a Grant in Aid for Scientific Research and the 21st Century Center of Excellence Program from the Ministry of Education, Culture, Sports, Science and

References

[1] K.N. Tu, J. Appl. Phys. 94 (2003) 5451.
[2]C.S. Hau-Riege, Microelectronics Reliability 44 (2004) 195.
[3] S. Vaidya, A.K. Sinha, Thin Solid Films, 75 (1981) 253.
[4] Y.-L. Chin, B.-S. Chiou, W.-F. Wu, Jpn. J. Appl. Phys., 41 (2002) 3057.
[5] B.S. Berry, A.C. Pritchet, J. Physique (Paris) 42 (1981) C5-1111.
[6] H. Mizubayashi, Y. Yoshihara, S. Okuda, Phys. Stat. Sol. (a) 129 (1992) 475.

[7] Y. Kabe, H. Tanimoto, H. Mizubayashi, Mater. Trans. 45 (2004) 119.
[8] H. Mizubayashi, K. Fujita, K. Fujiwara, H. Tanimoto, J. Metastable & Nanocrystalline Mater. 24-25 (2005) 61.
[9] N. Yagi, A. Ueki, H. Mizubayashi, H. Tanimoto, Journal of Metastable & Nanocrystalline Materials 24-25 (2005) 503.
[10] S. Sakai, H. Tanimoto, K. Otsuka, T. Yamada, Y. Koda, E. Kita, H. Mizubayashi, Scripta Mater. 45 (2001) 1313.
[11] H. Tanimoto, S. Sakai, E. Kita, H. Mizubayashi, Mater. Trans. 44 (2003) 94.
[12] Z.Q. Sun, T.S. Ke, J. Phys. (Paris) 42 (1981) C5-451.
[13] C.-K. Hu, L. Gignac, E. Liniger, B. Herbst, D.L. Rath, S.T. Chen, S. Kaldor, A. Simon, W.-T. Tseng, Appl. Phys. Lett. 83 (2003) 869.
[14] M.J. Kobrinsky, C.V. Thompson, J. Appl. Phys. 89 (2001) 91.
[15] D. Gan, P.S. Ho, R. Huang, J. Leu, J. Maiz, T. Scherban., J. Appl. Phys. 97 (2005) 103531.
[16] H.Tanimoto, K.Fujiwara, H.Mizubayashi, Science and Technology of Advanced Materials 6 (2005) 620.
[17] K. M. Latt, Y. K. Lee, T. Osipowicz, H. S. Park, Mater. Sci. Eng. B 94 (2002) 111.
[18] J.-W. Lim, K. Mimura, K. Miyake, M. Yamashita, M. Isshiki, Jpn. J. Appl. Phys. 42 (2003) 2780.
[19] R.S. Jones, J.A. Slotwinski, J.W. Mintmire: Phys. Rev. B 45 (1992) 13624.

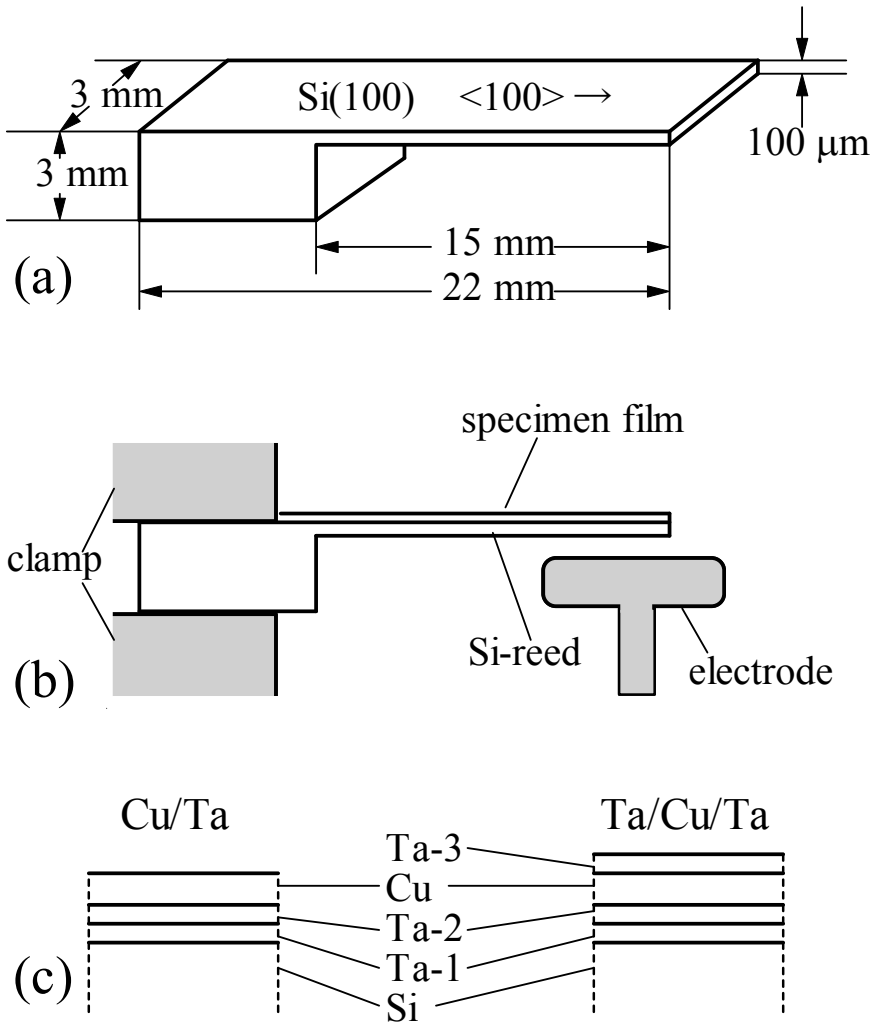

Fig. 1
Schematic diagrams : (a) a Si substrate, (b) a measurement setup, (c) cross sectional views of Cu/Ta and Ta/Cu/Ta films.

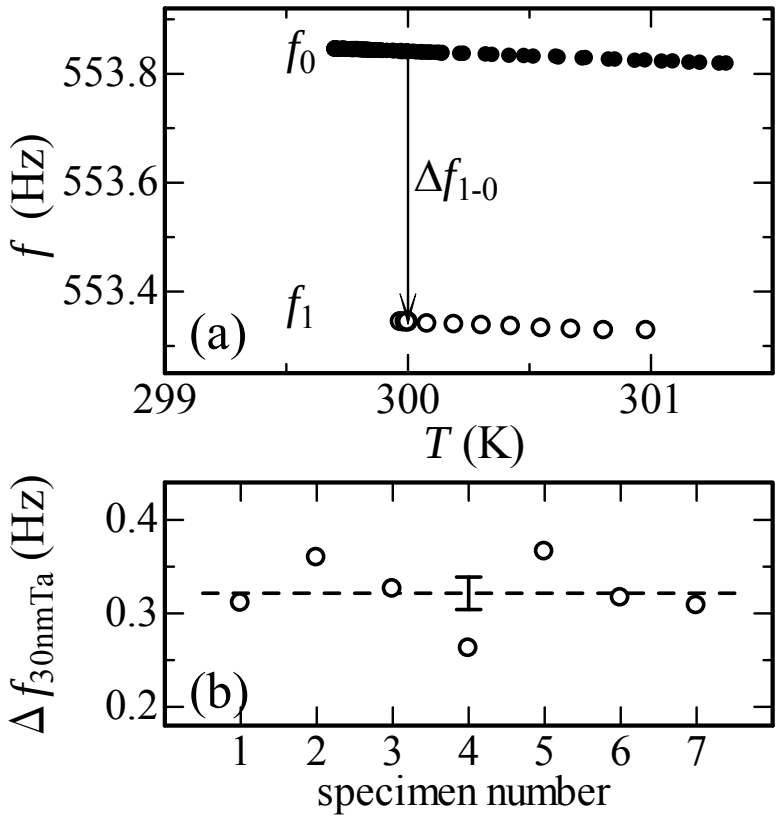

Fig. 2
(a) Examples for the *f* measurements: f_0 and f_1 were observed for a Si-reed with the Ta-1 layer and for the Si-reed after subsequent deposition of a 40 nm Cu specimen film following deposition of the Ta-2 layer, respectively. (b) Changes in *f* due to deposition of the 30 nm Ta-2 layer, $\Delta f_{30\text{nmTa}}$, measured for seven Si-reed specimens. See text for details.

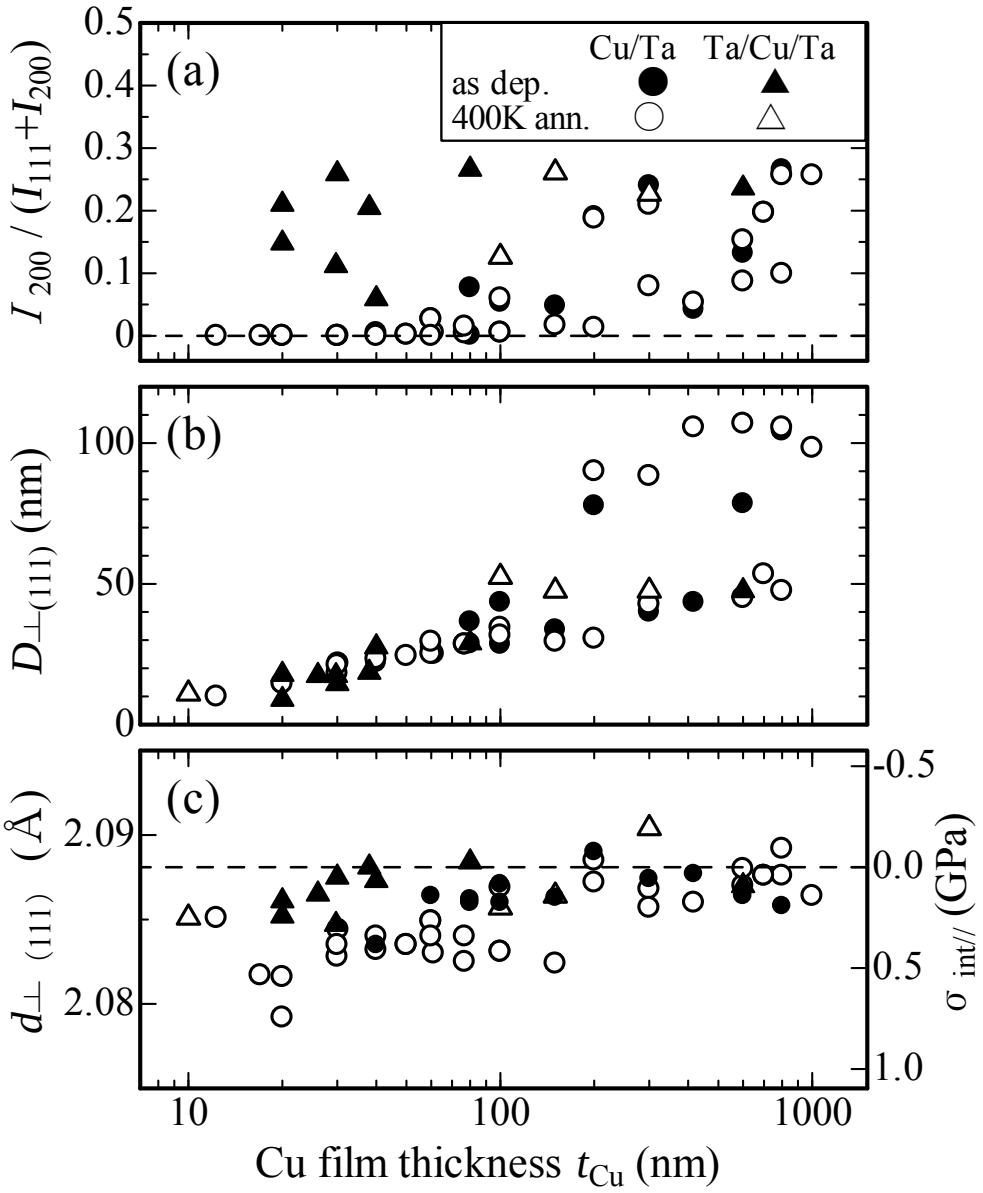

Fig. 3
The Cu film thickness (t_{Cu}) dependence of (a) the fractional intensity of the XRD 200 reflection, $I_{200}/(I_{111}+I_{200})$, (b) the mean grain size, $D_{\perp(111)}$, and (c) the (111) plane spacing, $d_{\perp(111)}$, observed for Cu/Ta films and Ta/Cu/Ta films. In (b), $D_{\perp(111)}$ was determined from the XRD (111) reflection and the Scherrer's equation. In (c), the internal tensile stress along the Cu film surface, $\sigma_{i//}$, was determined from the $d_{\perp(111)}$ data.

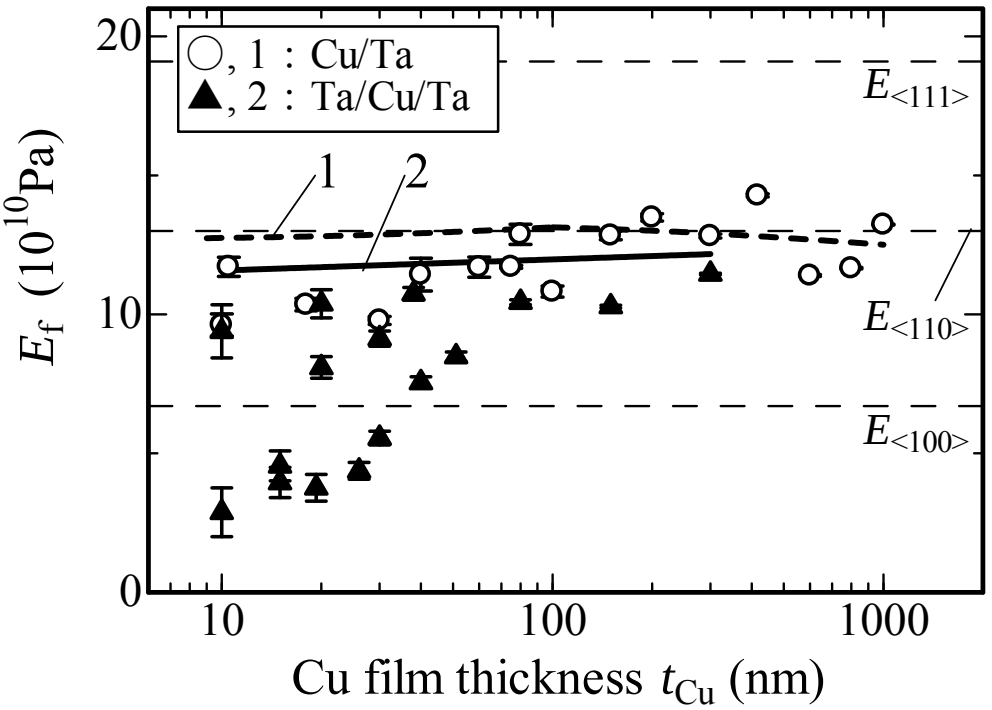

Fig. 4.
The E_f *vs.* t_{Cu} data observed for as deposited Cu/Ta films and Ta/Cu/Ta films. The dashed curve 1 and the solid curve 2 are the theoretical values of E_f estimated by taking into account the crystallographic texture (Fig. 3(a)) and the internal stress (Fig. 3(c)). $E_{<hkl>}$ indicates the Young's modulus of Cu along the <*hkl*> direction.

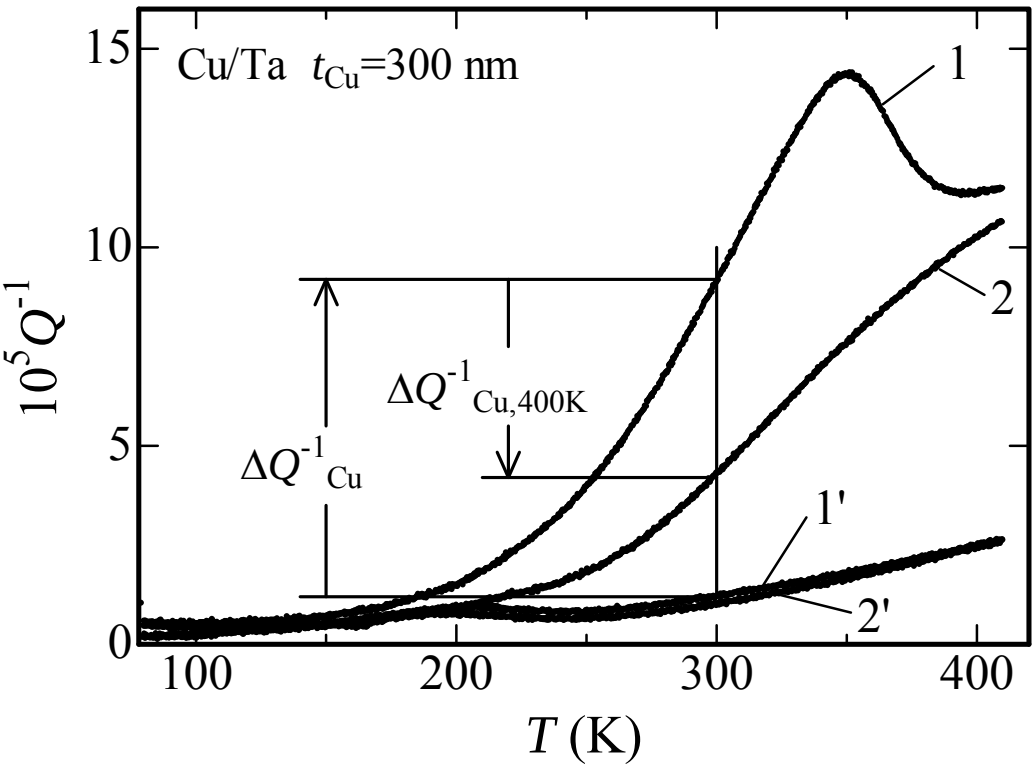

Fig. 5.
Examples of the Q^{-1} *vs*. T data observed for a Si-reed with a 30 nm thick Ta buffer layer alone in the as deposited state (1') and after warm up to ~400 K (2') and those observed for a Si-reed with a 30 nm thick Ta buffer layer and 300 nm Cu specimen film in the as deposited state (1) and after warm up to ~400 K (2).

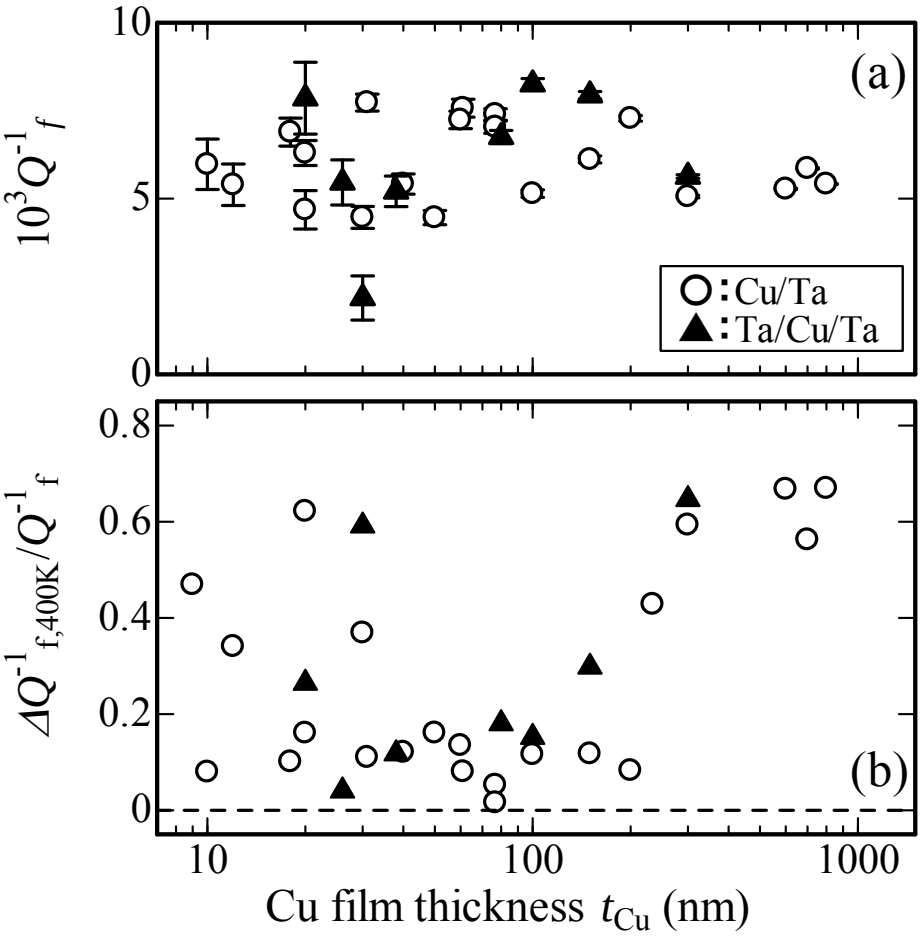

Fig. 6.
(a) The Q^{-1}_f *vs.* t_{Cu} data and (b) the $\Delta Q^{-1}_{f,400K}$ *vs.* t_{Cu} data observed at 300 K for Cu/Ta films and Ta/Cu/Ta films. See text for details.

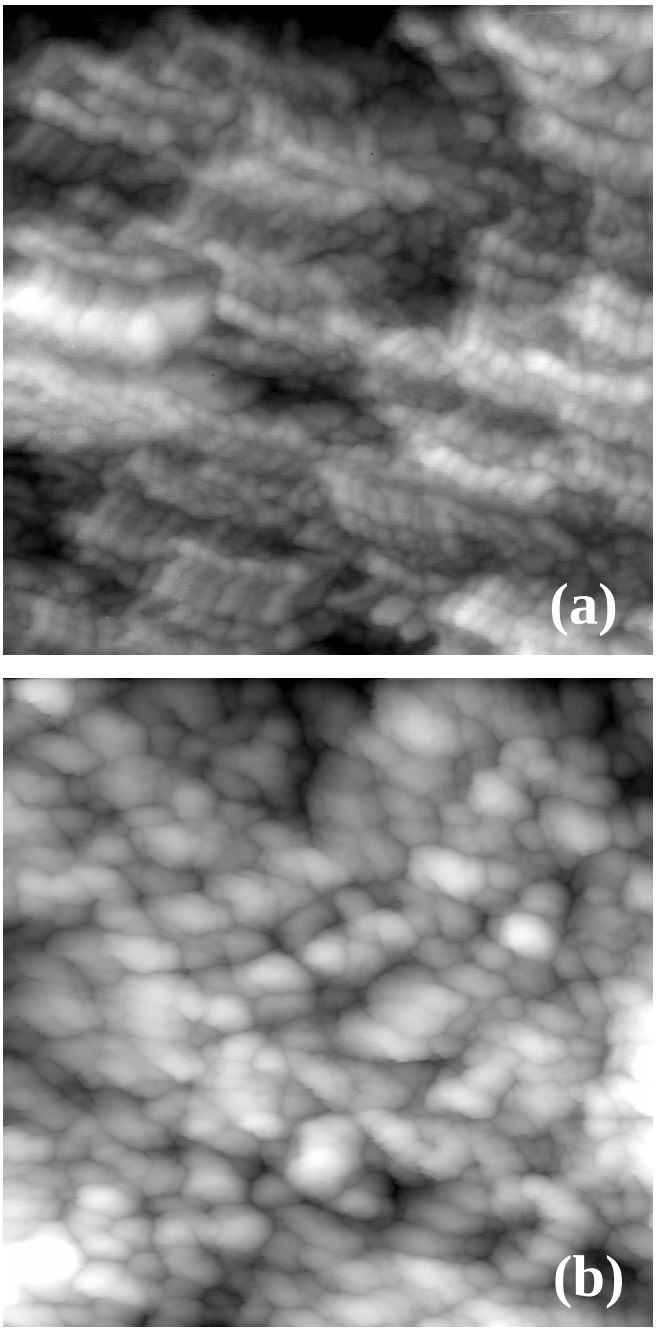

Fig. 7.
STM surface images for (a) a Cu/Ta film with t_{Cu} = 10 nm and (b) a Ta/Cu/Ta film with t_{Cu} =30 nm. The X-Y scale is 1000 nm and the height scale is about 50 nm for the both images.

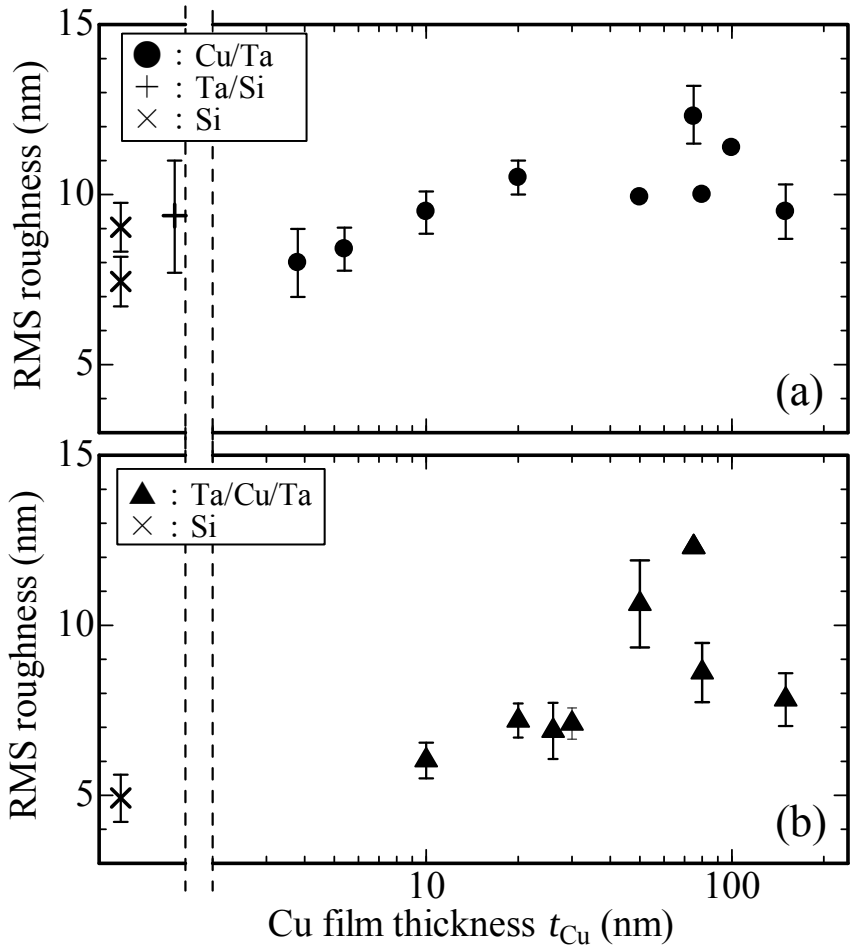

Fig. 8.
The Cu film thickness dependence of the root-mean-square (RMS) roughness estimated from the STM surface images for (a) Cu/Ta films and (b) Ta/Cu/Ta films. The data observed for a Si reed substrate after etching and a Si reed substrate with a 30 nm Ta buffer layer are also shown.